Subthreshold Pion Production in Heavy-ion Collisions

P. Hecking and G.F. Bertsch

The mechanism of the $\pi^{\pm}$-production in heavy-ion collisions below 200 MeV E/N is not understood. The thermal model and the first-chance collision model[1,2] (with a nuclear matter Fermi distribution) both underpredict the production by more than one order of magnitude at 100 MeV E/N. It was investigated, whether the change of the pion self-energy $\Pi(q,\omega)$ in the medium could be responsible for this discrepancy.

In a model of single N-N-collisions, a negative pion self-energy increases the N-N elastic and inelastic cross section, if single π-exchange between the nucleons dominates. Even with optimistic assumptions, however, this effect cannot increase the inelastic N-N cross section enough to obtain agreement with the experiment. On the other hand, the $\pi^{\pm}$- production rate in a thermal model is dominated by the factor $\exp(-\sqrt{k^2+m^2}-\Pi/kT)$. A negative self-energy would increase this factor. However, this correction gives only an upper bound of the number of pions, since in the medium they are off-shell, and they are partly reabsorbed in the NN-scattering process, which converts them into (finally measured) on-shell pions. Even with this upper bound, the thermal model cannot reproduce the experiment at energies as low as 100 MeV E/N.

So in both cases the pion self-energy cannot account for the discrepancies between theory and experiment. A model of single N-N collisions with a realistic momentum distribution of the nucleons is currently under consideration.

---

1. G.F. Bertsch, Phys. Rev. C15, 713 (1977).
2. W. Benenson, et al., Phys. Rev. Lett. 43, 683 (1979).

Analysis of Single Nucleon Spectroscopic Factors in the sd Shell

B.H. Wildenthal, W. Chung and K. Josafatsson

Shell model predictions for single nucleon transfer have been calculated for all sd-shell systems. Their predictions are being compared to the best average and best individual sets of experimental values in order both to evaluate the competency of the Chung-Wildenthal wave functions to comprehensively reproduce the details of these phenomena and also to determine the degree to which the existing experimental data, as reduced, are complete and internally consistent. The theoretical results are also being treated to extract occupation numbers, energy centroids and spreading widths. Preliminary results indicate that below A=28 the "particle" C-W wave functions reproduce experiment to better than 10% relative error in the matrix element (see Fig. 1). Above A=28, there are occasional disagreements of factors of two in large values, which correspond to misapportionment between two levels. Overall, however, the model continues to give an immediately recognizable image of the experimental facts.

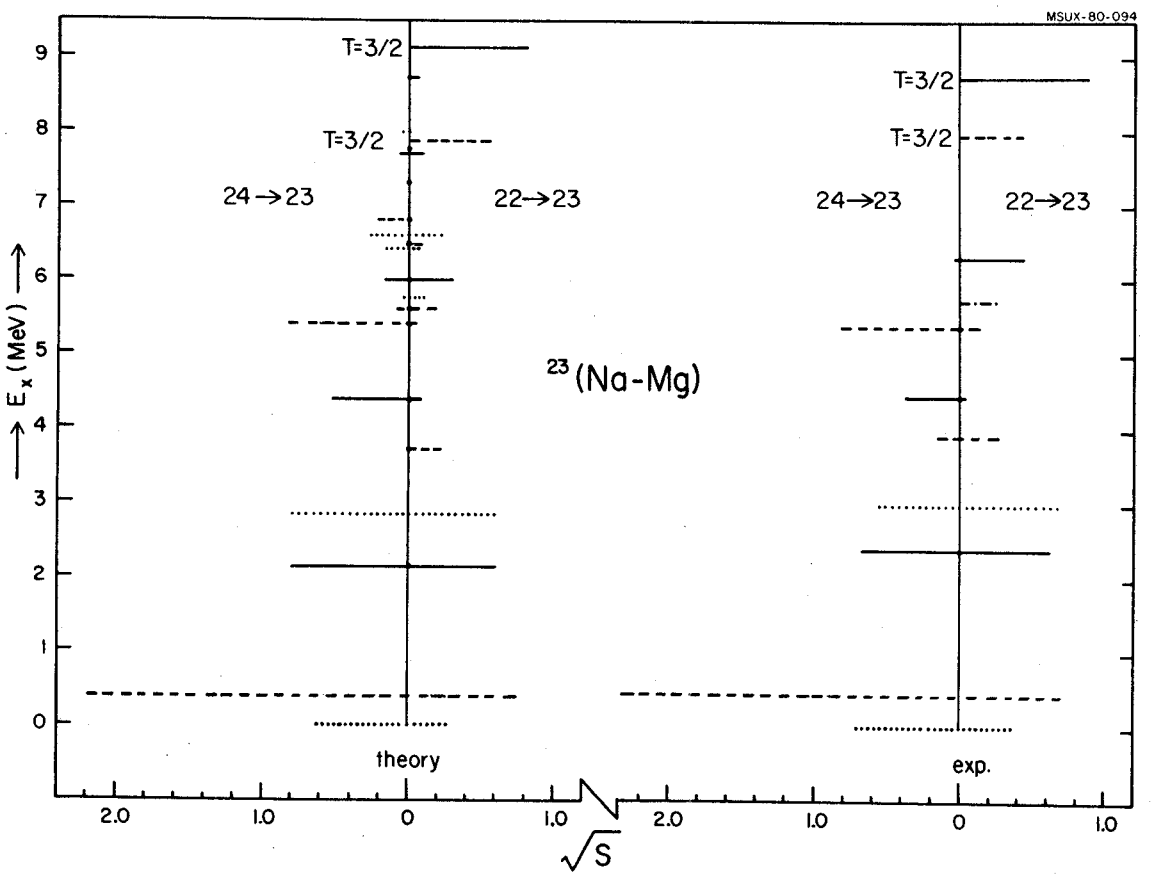

FIG. 1

Analysis of M1 Decay Widths in the sd Shell

B.H. Wildenthal, W. Chung, B.A. Brown
and J. Banks

The totality of magnetic dipole gamma ray decay decay data in the sd-shell has been collected and collated, using Endt and van der Leun, Nuclear Physics 310, as a base, and reduced to matrix elements $(2J_i+1)B(M1)$. These experimental data are being compared to each other to extract, where relevant, the isoscalar-isovector ratios and compared with theoretical matrix elements calculated from Chung - Wildenthal wave functions. This latter comparison is aimed first at elucidating the capability of the wave functions to reproduce small, highly cancelled matrix elements. To the degree that this appears possible, we will extract the values of the effective M1 single-particle matrix elements by which agreement between theory and experiment is optimized.

Some insight into the nature of isoscalar giant resonances can be gained by formulating the microscopic Random Phase Approximation (RPA) theory in terms of classical continuum variables. We have shown in earlier work[1] that the velocity field for monopole vibrations of large nuclear systems obeys the classical equations for an elastic medium. The concept of elasticity has now been applied to coherent quadrupole and octupole vibrations. Formulas based on classical vibrations of an elastic sphere are in excellent agreement with the quantum mechanical results for these states.

The assumption of coherent, small-amplitude harmonic motion about the self-consistent ground state leads to a compact variational expression for the frequency of vibration:

$$\omega^2 = \frac{I[\vec{u},\gamma,\psi_i^o]}{\frac{1}{2} m \int \rho_o \vec{u}\cdot\vec{u}\, d^3r}$$

The numerator is an integral over the self-consistent ground state which we identify as the potential energy associated with the displacement field $\vec{u}$. Comparison with the classical expression for this potential energy in an elastic medium yields approximate expressions for the Lamé coefficients, λ and μ, in terms of the properties of the interaction at equilibrium density.

We model the nucleus with a uniform elastic sphere. An elastic medium can support both longitudinal (compression) and transverse (shear) waves. The previously studied monopole vibrations are purely compressional modes, but higher multipolarity modes are complicated mixtures of longitudinal and transverse waves. The condition that the stress vanish at the free surface of the sphere determines the coupling of shearing and compressional motion.

The normal parity solution to the classical equations has the form:

$$\vec{u} = A\, j_{\ell-1}(q_\ell r)\vec{Y}_{\ell\ell-10} + \left(\frac{\ell+1}{\ell}\right)^{\frac{1}{2}} j_{\ell+1}(q_\ell r)\vec{Y}_{\ell\ell+10}$$
$$+ B\, j_{\ell-1}(q_t r)Y_{\ell\ell-10} - \left(\frac{\ell}{\ell+1}\right)^{\frac{1}{2}} j_{\ell+1}(q_t r)Y_{\ell\ell+10}$$
$$= u_-(r)Y_{\ell\ell-10} + u_+(r)\vec{Y}_{\ell\ell+10}$$

The precise values of the longitudinal and transverse wave numbers, q_ℓ and q_t, and the ratio of the coefficients A/B depend on the values of λ and μ through the boundary condition, and must be computed numerically. However, the lowest quadrupole and octupole vibrations turn out to be primarily transverse for all values of these parameters. The vibrational frequency is given by:

$$\omega^2 = \frac{\mu}{m\rho_o} q_t^2 = \frac{h^2 k_f^2}{5m^2} \frac{\gamma^2}{R^2}$$

The parameter $\gamma = q_t R$ varies by $\lesssim 2\%$ for $\mu \le \lambda \le \infty$. Looking at the formulas for the elasticity moduli we see that the energies of the quadrupole and octupole vibrations are almost independent of the compressibility.

The prediction of the classical elastic formulas are in excellent agreement with recent calculations for $\ell=2$ and 3 oscillation of large Fermi systems using an approximation to the full microscopic RPA theory.[2] Table I lists the calculated vibrational energies and the predictions of the elastic equations. Also shown is the result of the Tassie model (scaling), which assumes an incompressible, irrotational velocity field. The elastic formula is clearly closer to the full calculation and improves as A increases.

Table 1. Vibrational Energies (MeV)

A	ℓ	full calculation	Elastic	Scaling
208	2	9.5	9.35	10.5
	3	12.9	13.9	-
1000	2	5.6	5.4	6.4
	3	8.2	8.0	-

We directly compare the $\ell=2$ velocity fields in Fig. 1. The form of the dominant term, u_-, from the full calculation (dashed lines) is

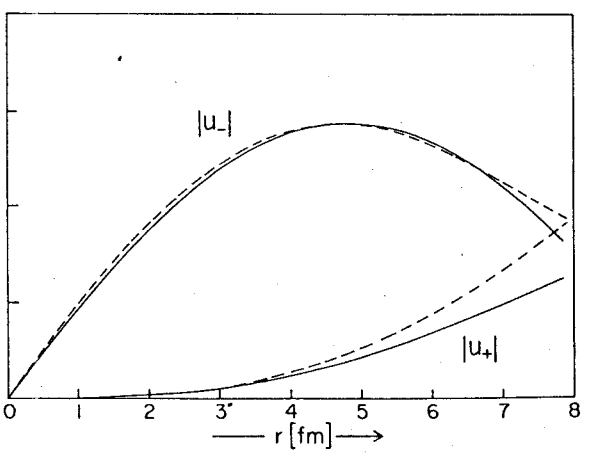

FIG. 1. The L=2 velocity fields for the giant quadrupole vibration in ^{208}Pb. The dashed line shows the Thomas-Fermi calculation of ref. (2), and the solid line shows the fields of classical elastic vibrations.

well reproduced by the elastic formulas (solid lines). While there is qualitative agreement for u_+, this term is more influenced by the true boundary condition at the nuclear surface, which is an increasing exponential. The velocity field is neither irrotational nor incompressible. The excellent agreement of the elastic formulas with the full calculations for the curl and divergence of $\vec{u}$ is shown in Fig. 2. Because $\nabla\cdot\vec{u}$ is small in the interior, the transition density is very close to Tassie form, even though the velocity fields are quite different.

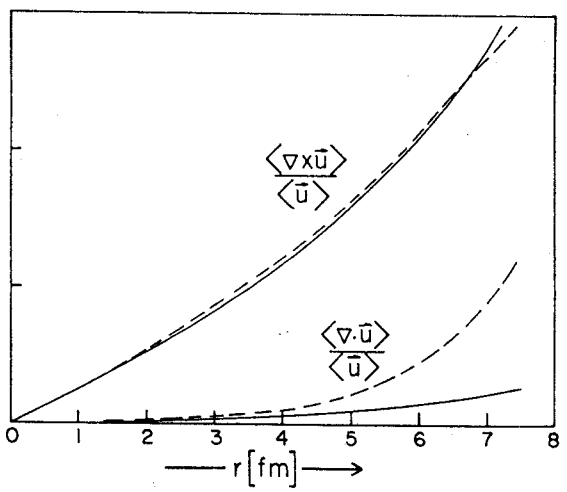

FIG. 2. The divergence and use of the velocity fields from Fig. 1.

We conclude that in quadrupole vibrations the motion of the bulk of the nucleons obeys the classical equations for an elastic medium. This also appears to be true for octupole vibrations, if we assume totally coherent motion. In actual nuclei, however, this assumption is probably not well satisfied.

---

1. F.E. Serr, G.F. Bertsch and J. Borysowicz, Phys. Lett. 92B, 241 (1980).
2. G. Eckart, G. Holzwarth and B. Schwesinger, Siegen Preprint, 1980, Phys. Lett. (to be published).

Spin Excitations in Nuclei

G.F. Bertsch

The recent measurements of spin excitations in nuclei via the (p,n) reactions make it possible to determine the spin dependent part of the effective interaction more accurately than was previously possible.

At 0^o the reaction makes a $\sigma\tau$ excitation, and the average energy of this state is directly related to the residual interaction. In Table I we quote experimental measured energies[1-3] for some magic nuclei. These numbers are mean energies of the upper component of the strength. In ^{90}Zr and ^{48}Ca, this includes a $T_>$ state as well as the giant Gamow-Teller state.

Table I. Energetics of Giant Gamow Teller States

	Nucleus		
	^{48}Ca	^{90}Zr	Pb
Experimental Excitation Energy	10.4 MeV[a]	9.3[b]	15.6[c]
(jj^{-1}) particle-hole excitation	-0.2 MeV	-0.1	3.6
Spin-Orbit Splitting	6.1 MeV	6.4	6.3
	Residual Interaction		
Empirical	4.5 MeV	3.0	5.7
G-Matrix	3.5 MeV	3.0	
G_0'	1.3	1.2	1.6

a) Ref. 1.
b) Ref. 2,3.
c) Ref. 4.

Much of the excitation energy is due to the spin-orbit splitting of the single-particle orbitals involved in the excitation. We estimate these using the Becchetti-Greenlees global spin-orbit potential. This is shown as the third line. The difference between the actual excitation and the single particle energy associated with a $(j_< j_>^{-1})$ configuration is the empirical residual interaction. This is shown as the fourth row in the table. We compare these numbers with the bare G-matrix of Ref. 5, shown as the fifth row, and find good agreement. Because G-matrix calculations are rather involved, it is worthwhile to find an equivalent δ-function interaction. The last column shows the strength of the δ-function interaction needed to reproduce the empirical energy. The interaction is expressed in terms of the Landau-Migdal parameter G_0', $v = G_0'\sigma_1\sigma_2\sigma_1\sigma_2\delta(r_1-r_2)$ x (150 MeV - fm^3).

The (p,n) experiments also locate L=1 strength,[6] presumably also associated with spin flip. We have made a similar analysis of the energetics of this state in ^{90}Zr. We find that there is a very large splitting between the centers of gravity of the 0^-, 1^- and 2^- strength functions. This is mainly due to the single particle spin-orbit splitting. Different orbitals dominate the strength function of different J states. The 0^- is highest because the configurations mostly involve a spin flip. The 2^- strength is lowest, with most contribution from orbitals differing by two units. In Table II we quote the results of preliminary calculation of the strength functions. We consider only the orbits of highest ℓ in each major shell, and use a delta function residual interaction with the strength given in Table I. The orbital excitation energy is taken to be 10 MeV. This is larger than the excitation energy in a Woods-Saxon well, following an effective mass of $\frac{m^*}{m} = 0.8$. The predicted excitation energy is lower than the measured energy. Either the effective mass could be smaller, or the G_1' interaction is significant.

Table II. The theoretical strength function for the $Y_1\sigma$ operator in ^{90}Zr.

	Relative Strength	Excitation Energy
$J = 0^-$	1	23 MeV
1^-	2.6	20
2^-	3.1	13
Average		17 MeV
Experimental		19 MeV

1. B.D. Anderson, et al., Phys. Rev. Lett. 45, 699 (1980).
2. D.E. Bainum, et al., Phys. Rev. Lett. 44, 1751 (1980).
3. W. Sterrenburg, et al., Proceedings of the International Conference on Nuclear Physics, Berkeley, 1980, p. 176.
4. D.J. Horen, et al., ibid., p. 272.
5. G. Bertsch, The Practitioner's Shell Model, North-Holland, 1972.
6. Proceedings of the International Conference on Nuclear Physics, Berkeley, 1980, pp. 175, 207, 241 and 272.

Knock-Out Description of Particle Emission in Heavy Ion Collisions

D. Cha and G. Bertsch

The pre-equilibrium emission of light particles is seen to be important at projectile energies greater than 10 MeV/nucleon.[1] A good fit to the energy spectrum is provided by a statistical model, with the temperature as a parameter.[2] It is of interest to compare also with direct knockout calculations, if a firm conclusion is to be drawn about the mechanism. We use the following equation to describe single-particle knockout:

$$\frac{d^3\sigma}{dk^3} \sim \int d^3k' [\, n_1(k'-p)V_2^2(k'+k-p) + n_2(k+k'-p)V_1^2(k'-p)] \, \delta(E_{k'}+E_{k+k'}+E_k-E_{in}) \quad (1)$$

In this equation p and k' are the initial and final momenta of the projectile, and k is the momentum of the knocked out nucleon. The function $n_i(q)$ is the momentum probability distribution of the nucleus i,

$$n_i(q) = (i|a_q^+ a_q|i). \quad (2)$$

The function $V_i(q)$ is the form factor of the nuclear potential in nucleus i,

$$V_i(q) = \int d^3r \, e^{iqr} V_i(r) \quad (3)$$

We shall apply the model to the measurements of protons from collisions of ^{16}O on ^{238}U (ref. 2), and we need to parameterize the functions n(q) and V(q) for these nuclei. The harmonic oscillator model gives a reasonable description of the ^{16}O Hartree-Fock wavefunction, and n(q) is easily evaluated as

$$N_{16}(q) = 4\left(\frac{b}{\sqrt{\pi}}\right)^3 (1+2b^2q^2)e^{-b^2q^2} \quad (4)$$

with b = 1.84 fm. If we assume a short range density independent interaction, V(q) is proportional to the density form factor, and is evaluated analytically as

$$V_{16}(q) = 4(4 - \tfrac{1}{2} b^2q^2)e^{-b^2q^2/4} \quad (5)$$

The functions n(q) and V(q) for ^{238}U should be similar to those for ^{16}O at high q, since this is a characteristic of the nuclear surface. In the calculation below we use the same functions for ^{238}U with b = 1.73 fm.

Before going on to the results of the knockout calculation, it is useful to make some qualitative observations. The shape of the energy spectrum from eq. (1) is determined to a fair approximation by the dependence of the integrand on k, since the boundary of the integral does not vary exponentially. Taking only the first term of the integrand in eq. (1), which dominates at forward angles, the k-dependence is given by

$$\frac{d^3\sigma}{d^3k} \sim e^{-(a_1k^4+a_2k^2+a_3k^3\cos\theta+a_4k\cos\theta)} \quad (6)$$

Here the constants a_i depend on the projectile energy and the form factor parameter b. We see from this that the knockout model should in principle be distinquishable from the thermal model, which demands a cross section behaving as

$$\frac{d^3\sigma}{d^3k} = e^{-c(k-k_0\cos\theta)^2} \quad (7)$$

We evaluate the integral (1) numberically without making the approximation (6) to compare the data measured recently by Gelbke, et al.[2] Before comparison can be made, we have to account for Coulomb effects on the energy. It seems reasonable to assume that the proton spectra would be shifted by the Coulomb energy at the contact point between the two nuclei. For ^{16}O on ^{238}U, this shift amounts to 20 MeV. The shifted results of eq. (1) are compared with the experimental data in Fig. 1. We have arbitrarily adjusted the overall normalization to fit the data. We see good agreement for the high energy tail of the spectrum and the angular distribution. However, the Coulomb shift is clearly excessive. A 10 MeV shift gives a much better fit, as is seen in Fig. 2. The overall quality of the fit, considering all of the data together, is about the same as the thermal model.

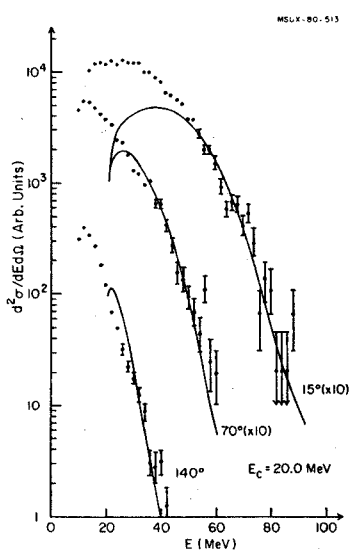

FIG. 1. A single nucleon knock-out model with E_c = 20.0 MeV.

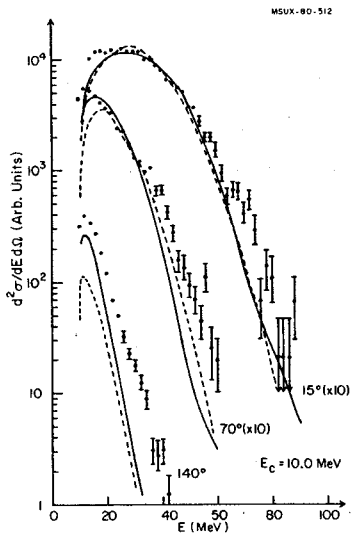

FIG. 2. A single nucleon knock-out model with E_c = 10.0 MeV. Solid line is from Eq. (1) and dashed line is from Eq. (6).

We have also considered two-nucleon knock-out as a possible mechanism for the reaction. The formula corresponding to eq. (1) when only one particle is observed, is

$$\frac{d^3\sigma}{dk^3} \sim \int d^3k' d^3k'' \; n_1(k'-p) n_2(k+k'+k''-p)$$

$$\delta(E_k+E_{k'}+E_{k''}+E_{k+k'+k''}-E_{in}) \qquad (8)$$

We find that this formula gives a much steeper slope in the energy spectrum, because n(q) decreases faster than V(q). The data are clearly incompatible with this mechanism.

Obviously there is much that remains to be done before we can put forward the single nucleon knockout as the mechanism for the reaction. A consistent calculaton requires distorted waves in the final state, and we have used plane waves in eq. (1). More difficult, but necessary to make a convincing case, the overall magnitude of the knockout should be calculated.

---

1. D.G. Sarantites, et al., Phys. Rev. C18, 774 (1978).
2. C.K. Gelbke, et al., Phys. Rev. Lett. 45, 513 (1980).

A Classical Model for Heavy Ion Collisions

G. Bertsch

We are formulating a classical model of heavy ion collisions. As far as we are able, the forces are based on known kynamic properties of nuclear matter. The variables we consider are the separation of the c.m. of the two nuclei, R_{sep}, and the radius of the neck joining the nuclei, R_{neck}. Once the geometry of the neck is known, the nuclear force between the nuclei can be obtained from the bulk properties of nuclear matter. We parameterize the neck evolution, guided by qualitative arguments and the results of TDHF calculations.

When the nuclei are not in contact, the force is taken to be the sum of a Coulomb force, a phenomenological nuclear potential, such as given in ref. 1, and a tangential force associated with particles tunneling from one nucleus to the other.[2] When the nuclei are in contact, the nuclear force is divided into a bulk component, equivalent to Randrup's friction force,[3] and a surface component given by

$$F = 2\pi R_{neck}\sigma \qquad \sigma \simeq 1 \text{ MeV/fm}^2 \tag{1}$$

We make simple assumptions about the evolution of the neck. When the two nuclei are coming together, the neck radius is determined from a geometic construction of overlapping spheres. When the nuclei draw apart, we assume that the rate of decrease of neck radius is proportional to the velocity of separation,

$$\dot{R}_{neck} = -\alpha \dot{R}_{sep} \tag{2}$$

This assumption is supported by TDHf calculations,[4] with $\alpha \approx \frac{1}{4}$. The reaction is assumed to end in fusion if $\dot{R}_{sep}$ goes to zero in the latter stage of the collision. We assume that the system undergoes scission when the neck radius becomes smaller than 1.4 fm. The neck can also break if the recession velocity of nuclei exceeds a critical value.[5] In practice we did not find that breakage occurs at low beam energies.

The Wilczynski for the model is compared with a TDHF calculation in Fig. 1. We see that the model minics the TDHF behavior quite well except in the more peripheral collisions. For these collisions the surface deformations are known to play a mojor role, and they are omitted from the model completely. Both TDHF and the model ahve a very strong deep inelastic scattering peak at c.m. energy of 250 MeV and scattering angle 40-50°. The peak is very easy to understand in the model. The energy loss can be calculated as the work done by the different forces. The Coulomb force is conservative and the volume nuclear force is relatively small. Most of the work is done by the surface force. This can be estimated as

$$2\pi\sigma \int R_{neck} dR_{sep} \simeq \pi\sigma \frac{(R_{neck}^{max})^2}{\alpha} \tag{3}$$

where R_{neck}^{max} is the maximum neck radius, attained at the point of closest approach. This maximum neck radius is rather insensitive to impact

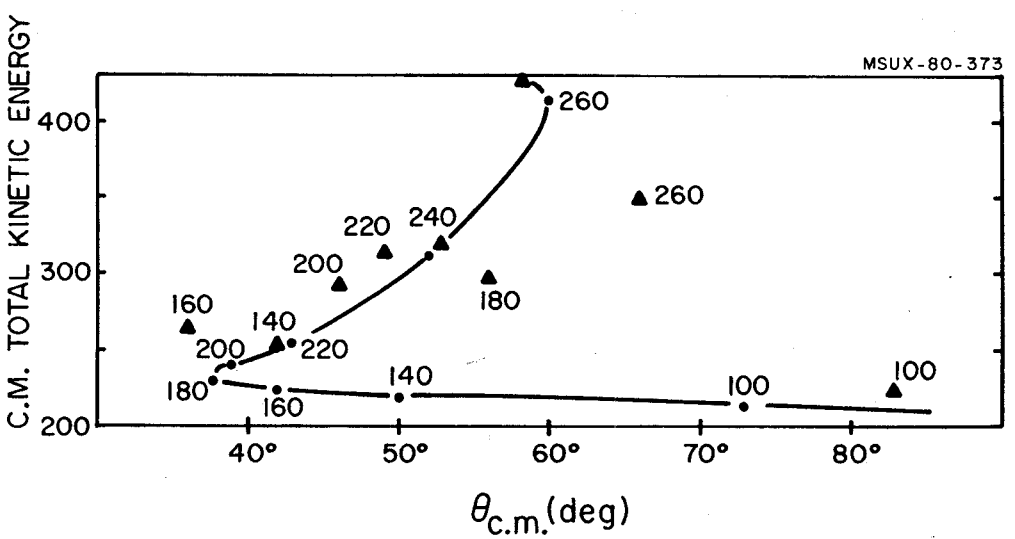

FIG. 1. Collision of $^{84}Kr + ^{209}Bi$ at energy E_{lab} = 600 MeV. The Wilczynski plot of c.m. energy vs. scattering angle is shown for the present model, with labeled dots showing points for specific values of the angular momentum. Corresponding points for the TDHF calculation of ref. (6) are shown as triangles.

parameter. Thus when eq. (3) is averaged over impact parameter, there remains a large peak.

The experimental data do not show as pronounced a deep inelastic peak as given by TDHF or this model. Nevertheless, it is instructive to have a more physical picture of the mechanism producing this peak.

1. R. Bass, Phys. Rev. Letters 39, 265 (1977).
2. C.M. Ko, et al., Phys. Letters 77B, 174 (1978).
3. J. Randrup, Ann. Phys. 112, 356 (1978).
4. A.K. Dhar and B.S. Nilsson, Phys. Letters 77B, 50 (1978).
5. G. Bertsch and D. Mundinger, Phys. Rev. C17, 1646 (1978).
6. K.T. Davies, et al., Phys. Rev. Letters 41, 632 (1978).